AIAA JOURNAL
Vol. 40, No. 4, April 2002

Determination of an Optimal Topology with a Predefined Number of Cavities

Hyunsun Kim*
University of Bath, Bath, England BA2 7AY, United Kingdom
Osvaldo M. Querin†
University of Leeds, Leeds, England LS2 9JT, United Kingdom
Grant P. Steven‡
University of Durham, Durham, England DH1 3LE, United Kingdom
and
Yi M. Xie§
Victoria University, Melbourne, Victoria 8001, Australia

In the field of topology optimization, increasing interest has been applied toward improving the practical applicability of the methods. Mechanically, a cavity in a structure introduces stress concentrations and, hence, structurally undesirable effects on the design. However, designs such as aircraft fuselages and wing ribs often require a specified number of cavities for their functional capabilities. Cavities also have the favorable consequence of reducing the weight. In this study, intelligent cavity creation is discussed as a means of determining an optimal topology with a desired number of cavities, based on evolutionary structural optimization. After the effect is shown on the total number of cavities when a new cavity is introduced during an optimization process, a parameter Γ is introduced that delays cavity creation. An investigation is carried out to observe the effects of various parameters such as Γ and mesh density on the final number of cavities.

Introduction

In recent years, the development of the optimization methods has focused on producing the best or optimum structure solely under structural criteria such as stress, stiffness, and weight.[1,2] However, as topology optimization has reached a level of maturity, interest is growing in the practical applicability of these methods. Some of these questions are manufacturability of the solution, checkerboard patterns, mesh dependency, and the incorporation of nonstructural constraints.

Manufacturability of an optimal topology may relate to various aspects of a design, such as the nature of an optimization method or the availability of manufacturing tools and technology. By the use of Aboudi microstructures or microcells with voids (see Refs. 1 and 3), a topology is represented with varying degrees of density values or perforated regions. To achieve a practical solution, the penalty technique is often employed to eliminate the intermediate densities.[4] The solid isotropic microstructure with penalty method[5] has been introduced as an alternative method that suppressed the perforated regions by relating the stiffness to the density of the isotropic material with a power greater than one. Another impractical feature commonly observed in optimal topologies is jagged edges.[6–8] These are due to the use of finite elements and do not represent the optimal features. Postprocessing using spline approximations and shape optimization has been suggested to obtain smooth outlines for these topologies.[9,10]

Presented as Paper 2000-4734 at the AIAA/NASA/USAF/ISSMO 8th Symposium on Multidisciplinary Analysis Optimization, Long Beach, CA, 6–8 September 2000; received 30 December 2000; revision received 27 August 2001; accepted for publication 27 August 2001.

*Aerospace Engineering Lecturer, Department of Mechanical Engineering; h.a.kim@bath.ac.uk. Member AIAA.
†Lecturer, School of Mechanical Engineering. Member AIAA.
‡Professor, School of Engineering, South Road.
§Associate Professor, School of the Built Environment, P.O. Box 14428.

A checkerboard pattern describes a region of alternating solid and void elements in a topology and is commonly found in optimal solutions. It has been proven that the formation of the checkerboards is due to numerical instability and does not represent an optimal feature of the design.[11,12] Following on from this discovery, several methods have been introduced to eliminate or prevent the formation of the checkerboard patterns.[13] It has been shown that the use of higher-order finite elements mostly prevents checkerboarding[11,12]; however, this is at the expense of the computational cost. An alternative and computationally cheaper method is to use a weighted average of the design sensitivity[14] or elemental density[15,16] over an element and its neighbors.

It has been seen that reducing mesh dependency also reduces checkerboarding.[13,17] The mesh independent filtering suggested by Sigmund is an extension of the checkerboard filter using the weighted averages of elements, which was mentioned earlier.[14] The method uses the element sensitivities computed by weighted averages based on the distances between elements and has been shown to produce mesh-independent designs.

Another technique that produces mesh-independent results is to introduce a local gradient constraint on element density variation. Petersson and Sigmund[18] have been able to prove that the gradient constraint not only ensures existence of a solution but also prevents the formation of checkerboards. However, the algorithm is considered to be computationally demanding due to the large number of constraints.

The perimeter method imposes an additional constraint on the perimeter, which is the sum of the circumferences of the internal boundaries.[19] A checkerboard can be viewed as a region of numerous holes, and the number of holes is proportional to the total perimeter. Thus, by introducing an upper bound to the total perimeter, it effectively reduces the number of holes that can be created and, hence, reduces checkerboards and mesh dependency. The perimeter method has been extended to three-dimensional optimization problems.[20]

A common feature of the preceding three methods (i.e., mesh independent filtering, local gradient constraints, and perimeter method) is their potential ability to incorporate a sizing requirement as a design constraint. Sizing requirements are often determined by nonstructural concerns such as manufacturing technology,

functions, and aesthetics. In engineering designs, some of these constraints may be more critical than the structural constraints.

Mesh independent filtering has been shown to be efficient in minimum member size control, although it is not applicable to multiple constraint optimization problems.[17] The local gradient constraint method, however, has successfully been extended to minimum member size control problems with multiple constraints. Zhou et al.[17] were able to impose the minimum member radius using a density slope constraint and found more manufacturable solutions.

A direct consequence of the local gradient constraint on the element densities is that it imposes an upper bound to the design oscillations and, consequently, the maximum number of cavities.[18] Similarly, the perimeter constraint reduces the number of cavities in an optimal topology, thereby preventing a checkerboard formation.[19] Although these methods have the potential to control the number of cavities, the bounds or values of these parameters that lead to a desired number of cavities are not known.

Intelligent cavity creation (ICC) attempted to control the number of cavities in an optimal topology.[21] Based on evolutionary structural optimization[2] (ESO), ICC controls when the cavity is created during optimization. The method starts from the full design domain with no cavities and creates cavities as needed. Thus, when the number of cavities reaches a desired number, ICC no longer creates cavities but continues optimizing the existing boundaries, that is, topology optimization becomes shape optimization. It has been demonstrated that delaying the cavity initiation reduces the maximum number of cavities in the final topology. As in the perimeter control method, ICC also prevents the formation of checkerboards.

A further investigation on the ICC algorithm is carried out and presented in this paper, aimed to obtain guidelines for the selection of the initial parameters for a desired number of cavities. During the study, the ICC algorithm was modified to improve its effectiveness. The next section explains the original formulation of ICC, followed by a section outlining the modifications and the revised ICC method. The effects of the various parameters such as optimization rate and mesh density on the final topology are then studied and discussed. The results indicate a relationship between the parameters and the number of cavities and provide a guide for selecting the parameters.

Original Formulation of ICC

It is proposed that there exists a set of optimal topologies for a given design problem, with a varying number of cavities.[21] Original ESO finds the solution with the maximum number of cavities whereas nibbling ESO finds the solution with no cavities.[2]

The previous formulation of ICC is a hybrid of these two methods: original ESO and nibbling ESO. Nibbling ESO is applied to optimize only the boundaries of a structure. At the end of each iteration, the stress values inside the structure are examined to determine the need for a cavity. If a low-stress region inside the structure has stress below a predefined threshold, then it is said that there is a need for a cavity. In such a case, original ESO is applied to initiate an internal cavity. After creating a new cavity, nibbling ESO is continued to modify the boundaries until there is a need for another cavity.

The need for a cavity is measured by insert cavity ratio (ICR), which is a function of the current stress state and changes as the structure is evolved, [Eq. (1)]. When this value is less than or equal to the predefined threshold cavity creation number Γ, a new cavity is initiated. Note that for stress-based ESO, the optimization-driving criterion is commonly the elemental von Mises stress:

$$\mathrm{ICR} = \frac{\sigma_{\mathrm{VM\,min}}}{\sigma_{\mathrm{VM}\,b,\mathrm{min}}} \tag{1}$$

where $\sigma_{\mathrm{VM\,min}}$ is the minimum criterion of nonboundary elements and $\sigma_{\mathrm{VM}\,b,\mathrm{min}}$ the minimum criterion of boundary elements.

Modified Formulation of ICC

Definition of ICR

A stress distribution of a domain can be represented three dimensionally as in Fig. 1, where, in this case, a low-stress region and hence a need for a new cavity, is recognized at A. However, one may encounter cases where the boundary stress is lower than the nonboundary stress that is less than the deletion criterion. Such a

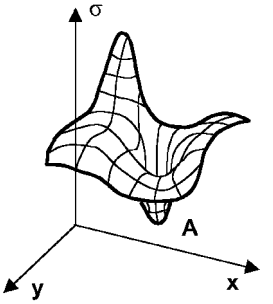

Fig. 1 Example of stress distribution.

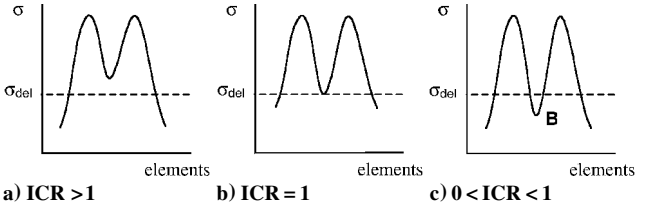

Fig. 2 Two-dimensional stress distributions.

distribution is depicted in Fig. 2c, in the simplified two-dimensional space where there is a need for a new cavity at B. However, due to the low boundary stress, ICR can still be greater than one, and the need for new cavities is not recognized.

Thus, a new definition of ICR is introduced. In contrast to the previous definition that was a function of boundary stress values, the new definition is a function of the deletion criterion. Here, only the magnitudes of the stress are of interest, and, hence, the absolute values are used to account for negative stresses:

$$\mathrm{ICR} = |\sigma_{\mathrm{nb}}/\sigma_{\mathrm{del}}| \tag{2}$$

where σ_{nb} is the minimum stress of nonboundary elements and σ_{del} is the deletion criterion below which all elements are removed.

As a structure is evolved, the value of ICR changes and, thus, is calculated at every iteration. If this value is greater than one, the stress distribution can be depicted in two dimensions as in Fig. 2a, where all stress values inside the structure are greater than σ_{del}, and, hence, there is no need for a cavity.

When ICR = 1, the minimum nonboundary stress value equals to σ_{del} (Fig. 2b). If, at this point, inside elements are allowed to be removed, all elements with the stress value of σ_{del} or less would be removed, and, thus, it can be said that the optimization technique is equivalent to original ESO.

When $0 < \mathrm{ICR} < 1$ such as in Fig. 2c, there is at least one point inside the structure where the stress value is less than σ_{del}. Original ESO immediately removes the elements with stress $\leq \sigma_{\mathrm{del}}$; thus, this stress state would not normally be observed. However ICC controls when a cavity is to be created, where the lower ICR value represents an increased need for a cavity.

The value of ICR is compared with Γ to determine the need for a cavity. A cavity is created if the ICC inequality (3) is satisfied:

$$\mathrm{ICR} \leq \Gamma \tag{3}$$

where Γ is the cavity creation number, $0 \leq \Gamma \leq 1$.

The value of ICR indicates the need for a cavity, which increases as ICR decreases. Hence, the delay mechanism for a cavity creation is controlled by the magnitude of Γ, with the level of delay being inversely proportional to Γ. Note here that when Γ is set to 0, the ICC inequality cannot be true; therefore, a cavity will not be created. Therefore, ICC with $\Gamma = 0$ is equivalent to nibbling ESO.

Starting a Cavity

The preceding ICC method employs original ESO[22] to initiate a cavity, where elements are removed according to the ESO inequality (4):

$$\sigma_{\mathrm{VM},e} \leq \sigma_{\mathrm{Del\,Crit}} \tag{4}$$

where $\sigma_{\mathrm{Del\,Crit}}$ is the deletion criterion, RR $\times\, \sigma_{\mathrm{VM,max}}$; RR the rejection ratio[2]; and $\sigma_{\mathrm{VM},e}$ the selected criterion of element e.

When the optimization technique is switched during an evolutionary process and an immediate initiation of a cavity is desired, RR must be determined such that a cavity is created immediately, and this is not an obvious task.

However, when a new cavity is required, the location for a new cavity is known, namely, where the minimum nonboundary stress occurs. Therefore, when a new cavity is needed, a new deletion criterion is calculated according to Eq. (5) instead of the original ESO formulation (4):

$$\sigma_{\text{del}} = |\sigma_{\text{nb}}| \times (1 + \text{RR}_C) \tag{5}$$

where RR_C is the rejection ratio set to a small number, typically 0.001.

The new definition of the deletion criterion is a value slightly greater than the minimum stress of the nonboundary elements. This ensures an immediate initiation of the cavities at the minimum stress locations in the structure. Furthermore, if there were more than one minimum stress location, which would be the case in symmetrical structures, an appropriate number of cavities would be created with a few elements per cavity. It also follows that one iteration would suffice to initiate the cavities.

After creating an appropriate number of cavities, nibbling ESO is continued with the earlier evolutionary rate constants. This allows further modifications of the boundaries including the boundary of any new cavities until the stress distribution is such that there is a need for more cavities.

Modified Methodology of ICC

When a design problem is defined, a finite element analysis (FEA) is carried out on the design domain, providing the stress values to determine which boundary elements are to be removed. Up to this point, it follows nibbling ESO. However, at the end of a steady state, ICR is calculated and compared with Γ to determine whether a cavity is required. If the ICC inequality (3) is not satisfied, nibbling ESO is continued. If there is a need for a cavity, a new deletion criterion is calculated according to Eq. (5), and all boundary and nonboundary elements below the new deletion criterion are removed.

After starting a cavity, the number of new cavities is counted, and nibbling ESO is continued again until another need of new cavities arises. When the current number of cavities reaches the required number of cavities initially specified by the user, then there is no need to create any more cavities. Thus, nibbling ESO is continued without calculating ICR until the optimum is found and/or all of the specified criteria are met.

The step-by-step process of the ICC algorithm is outlined hereafter and summarized in Fig. 3:

1) Define the design problem and specify kinematic constraints and material properties. Specify the number of cavities required in the structure and a value for Γ.

2) Start nibbling ESO.

3) When a steady state is reached, check whether all design constraints are met. If all design constraints are met and an optimum is reached, terminate the optimization process here, otherwise continue to step 4.

4) Compare the current number of cavities with the specified required number of cavities. If there are enough cavities, then go back to step 2 and continue nibbling ESO.

5) If there are not enough cavities, calculate the value of ICR and compare it with Γ. If ICR is greater than Γ, go back to step 2 and continue nibbling ESO, otherwise continue to step 6.

```
Define design problem;
do while (optimum is not reached)
    Nibbling ESO;
    if (current number of cavities < specified)
        Calculate ICR;
        If (ICR ≤ Γ)
            Start a cavity;
        end if,
    end if,
end do,
```

Fig. 3 ICC algorithm.

Table 1 Initial stress states of short cantilever beam

Mesh	Maximum stress	Mean stress	Mean/maximum stress ratio
48×30	12.86	3.350	0.261
64×40	17.07	3.354	0.197
80×50	21.30	3.356	0.158
96×60	25.53	3.358	0.132
112×70	29.77	3.359	0.113

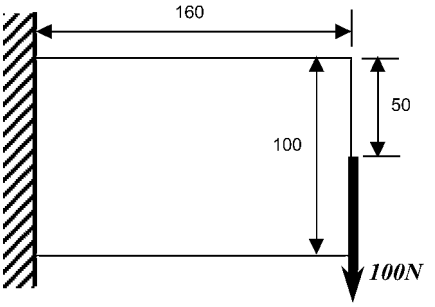

Fig. 4 Short cantilever beam design problem.

6) To create a cavity, first calculate the deletion criterion (5). Then remove all elements with stress values below the deletion criterion value. After creating a cavity, go back to step 2.

Investigation of Optimization Parameters and Number of Cavities

ICC controls when a cavity is initiated by varying Γ. However, there are other optimization parameters such as the mesh density and ESO driving criterion. The effects of various initial parameters on the optimum solutions are investigated and the results are discussed in this section.

Optimization of Short Cantilever Beam

Problem Definition

A short cantilever beam of aspect ratio 1.6 is optimized using ICC with varying parameter values. The beam is built in at the left-hand side and a 100-N downward force is applied in the middle of the right-hand end, as shown in Fig. 4. The material property of steel is assumed and plane stress/strain elements are used to model the problem. The ESO driving criterion was elemental von Mises (VM) stress. The varied parameters are optimization-driving criterion of maximum and mean stress, mesh density, and Γ. Table 1 summarizes the initial stress state for various mesh density.

The optimal topologies are selected by considering two factors: volume and the ratio of the mean over maximum VM stress. Topologies with a volume reduction of around 40% are considered for comparison. The stress ratio represents the evenness in the distribution of VM stresses, and, for a fully stressed design, the higher stress ratio value is preferred. Ideally, the stress ratio should trend upward to unity, but due to local high stresses at supports and load application points this rarely happens with FEA (Table 1).

Optimization Driving Criterion

The maximum VM stress and the mean VM stress are selected for the optimization-driving criteria. Using the mean VM stress as an optimization-driving criterion means that when calculating the deletion criterion in Eq. (4), the mean VM stress value is multiplied by RR, instead of the maximum VM stress. Two mesh densities are used: 64×40 and 112×70. The value of Γ is set to 1.0, creating the maximum number of cavities for the given conditions.

As can be seen in Table 1, the calculation of the maximum VM stress depends greatly on the mesh density due to the singularity near the point loads and supports in the FEA formulation. Table 1 suggests that the maximum VM stress is approximately linearly proportional to the mesh density. However, the mean VM stress does not vary greatly as the mesh density increases. It follows, therefore, that optimization driven by the maximum VM stress is more mesh dependent than the one by the mean VM stress.

Table 2 Optimality comparison of maximum and mean VM stress as driving criteria

Mesh	Criteria	σ_{del}	Volume, %	Maximum stress	Mean stress
64 × 40	Maximum	3.60	43.6	19.66	6.98
112 × 70	Maximum	4.18	37.2	30.76	8.26
64 × 40	Mean	3.58	44.7	19.59	6.83
112 × 70	Mean	3.82	40.6	30.64	7.66

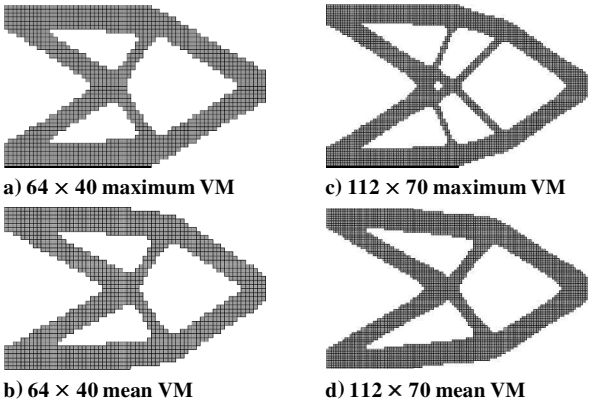

Fig. 5 Optimal topologies with varying optimization driving criteria.

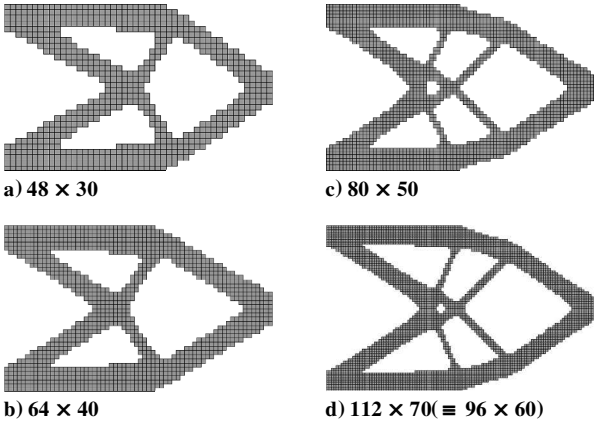

Fig. 6 Optimal topologies with varying mesh densities.

This mesh dependency characteristic can be seen in Fig. 5. For mesh 64 × 40 and 112 × 70, the optimal topologies obtained by the mean VM stress produce more mesh independent results than those by the maximum VM stress.

Table 2 summarizes the optimality of the four optimal topologies. The stress states of the optimal topologies show that comparable optimal states are reached by all optimizations. The volume ratio values indicate that it is possible to obtain topologies of less volume with the maximum VM stress solutions; however, the quantitative advantage is only slight.

Mesh Density

For optimization with varying mesh densities, the optimization driving criteria used was the maximum VM stress, the most commonly used criteria for ESO. The Γ value was set to 1.0. Five mesh densities were applied: 48 × 30, 64 × 40, 80 × 50, 96 × 60, and 112 × 70.

Figure 6 depicts the optimal topologies for the varying mesh density. As the mesh density increased, the number of cavities also increased. However, for the same number of cavities, the optimal topologies are comparable despite the differing mesh densities (Figs. 6c–6e). Also, for a finer mesh, an optimal topology with less volume can be obtained, hence, it can be said that a finer mesh leads to more refined optimization.

Table 3 summarizes the optimality of the optimal topologies of Fig. 6. The stress states of the optimal topologies show that they all

Table 3 Optimality comparison of varying mesh densities

Mesh	σ_{del}	Volume, %	Maximum stress	Mean stress
48 × 30	3.70	44.03	17.20	6.80
64 × 40	3.60	43.59	19.66	6.98
80 × 50	3.87	41.25	22.40	7.40
96 × 60	3.96	40.69	26.73	7.56
112 × 70	4.18	37.17	30.76	8.26

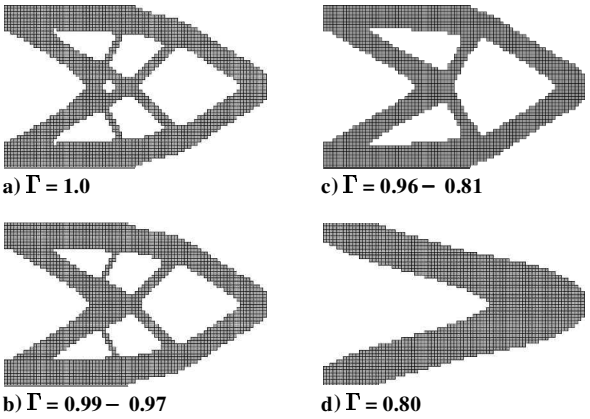

Fig. 7 Optimal topologies with varying Γ.

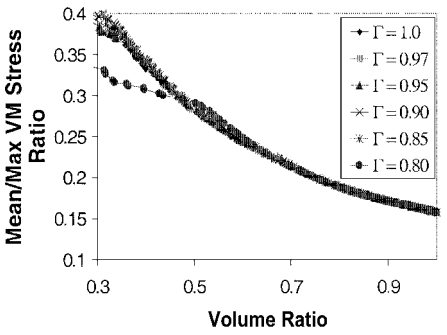

Fig. 8 Evolutionary history of topologies with varying Γ.

have reached comparable optimal states. The maximum VM stress of the final topology still increases as the mesh density increases. However, relative to their initial state, the maximum VM stress of the mesh density 48 × 30 increased by 33.8%, whereas that of 112 × 70 increased only by 3%.

For each mesh density, ICC is applied several times with varying Γ values. Whereas the number of cavities increase with mesh density at $\Gamma = 1.0$, the range in which ICC created cavities decreases with mesh density. For mesh 48 × 30, three cavities are obtained at $\Gamma = 0.80$, and no cavities are created when $\Gamma = 0.75$. However, for mesh 80 × 50, no cavities are created at $\Gamma = 0.80$. This is due to the more refined optimization, where for a high mesh density, the stresses are more evenly distributed and, hence, a "better" optimum is obtained. Thus, a lower value of ICR can be obtained in a coarse mesh, leading to a larger range of a possible Γ values that create cavities.

Cavity Creation Number Γ

For the 80 × 50 mesh, the short cantilever beam was optimized, driven by the maximum VM stress. Γ was set to values between 1.0 and 0.80 at an interval of 0.01.

The topologies in Fig. 7 are obtained at a volume of approximately 45%. When $\Gamma = 0.80$, no cavities are created and the optimization process is equivalent to nibbling ESO. Thus, the evolutionary history of this topology is quite different from the other solutions and the difference in the optimality and the stress states as shown in Table 4. However, the other topologies have reached a comparable optimality. This is also reflected in the evolutionary histories of these topologies (Fig. 8). Despite the differences in the final topologies,

Table 4 Optimality comparison of varying Γ

Γ	Cavities	σ_{del}	Volume, %	Maximum stress	Mean stress
1.0	6	3.60	45.2	22.39	6.837
0.99–0.97	5	3.54	45.3	22.39	6.822
0.96	3	3.47	45.3	22.26	6.865
0.95–0.93	3	3.45	45.2	22.27	6.887
0.92	3	3.43	44.8	22.25	6.937
0.91	3	3.45	45.5	22.25	6.860
0.90	3	3.47	45.2	22.25	6.892
0.89–0.87	3	3.45	45.5	22.24	6.864
0.86	3	3.51	45.2	22.24	6.914
0.85–0.84	3	3.47	45.3	22.24	6.888
0.83	3	3.49	45.2	22.23	6.910
0.82	3	3.42	45.2	22.23	6.900
0.81	3	3.42	45.2	22.23	6.894
0.80	0	3.85	43.6	25.18	7.554

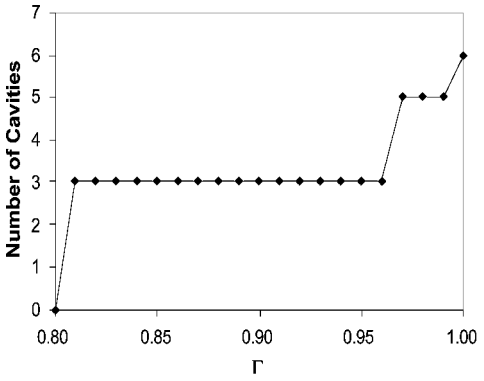

Fig. 9 Number of cavities vs Γ.

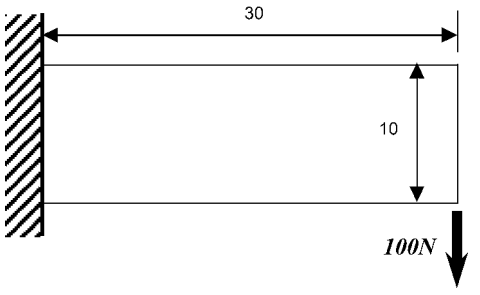

Fig. 10 Problem definition of cantilevered beam of aspect ratio 3.

they follow the same evolutionary path until too much material is removed and the solutions become numerically unstable. The evolutionary history of the nibbling ESO solution, however, deviates from the other evolutionary paths earlier on due to the prevention of a cavity creation.

As the value of Γ decreases, the number of cavities decreases in general as displayed in Fig. 9. This is demonstrated in Figs. 7b and 7c, where the exact same optimum solution is reached although the Γ values were different. Furthermore, the Γ values from 0.96 to 0.81 produced the same number of cavities, and their topologies are very similar. The stress states and the evolutionary histories suggest only a slight variation of optimalities among these topologies. Thus, it can safely be said that the topologies with the same number of cavities are of an equivalent optimum for practical purposes and the differences are insignificant. Also note that there exists a bound of mesh density and the Γ values of which lead to the same number of cavities.

Optimization of Cantilevered Beam of Aspect Ratio 3

Problem Definition

A cantilevered beam of aspect ratio 3 is optimized. The beam was built in at the left, and a 100-N downward force is applied at the bottom right tip as shown in Fig. 10. Again, the material property of steel is set and four-node plate elements are used to model the problem. The maximum VM stress is selected for the ESO driving criterion. Mesh density and Γ values are varied. The optimal topologies are selected at an equivalent volume level of around 53%.

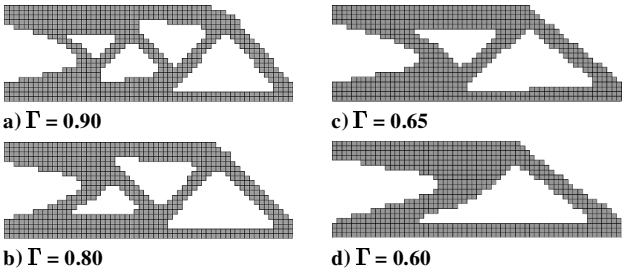

Fig. 11 Optimal topologies with varying Γ for 60 × 20.

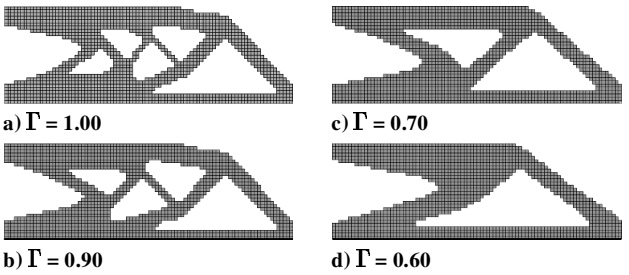

Fig. 12 Optimal topologies with varying Γ for 90 × 30.

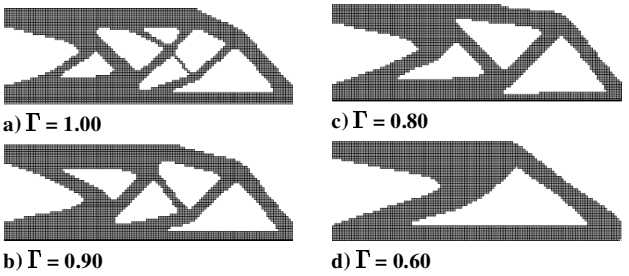

Fig. 13 Optimal topologies with varying Γ for 120 × 40.

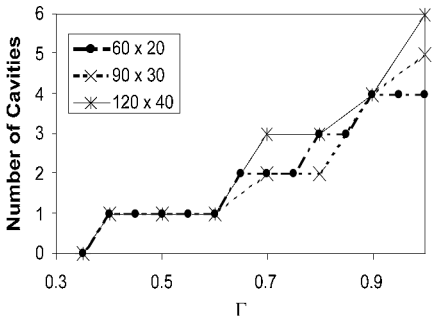

Fig. 14 Number of cavities vs Γ.

Results

Three different mesh densities were tested: 60 × 20, 90 × 30, and 120 × 40. For the mesh of 60 × 20, Γ was from 1.0 to 0.35 at intervals of 0.05, and, for the other mesh densities, Γ varied from 1.0 to 0.30 at intervals of 0.10. Figures 11–13 summarize the optimal topologies.

Similarly to the first example, the number of cavities increases with mesh density and Γ values as displayed in Fig. 14. For a smaller element size, a smaller amount of material can be removed at each iteration, leading to a more refined optimization and, hence, a greater number of cavities in the optimal topology.

The other parameter considered for this example is the Γ values, as summarized in Fig. 14. For all three mesh densities, no cavities are created for Γ less than or equal to 0.35. Table 5 suggests that

Table 5 Summary optimality of beam: aspect ratio of 3

Γ	σ_{del}	Volume, %	Maximum stress	Mean stress	Mean/maximum stress ratio	Number of cavities
			Mesh 60 × 20			
1.00	23.21	53.1	125.47	45.37	0.362	4
0.95	23.20	52.9	125.43	45.52	0.363	4
0.90	22.66	53.0	121.84	45.43	0.373	4
0.85	23.65	53.1	129.26	45.81	0.354	3
0.80	22.42	53.4	122.53	45.63	0.372	3
0.75	23.59	52.9	129.60	46.27	0.357	2
0.70	23.60	52.9	130.38	46.20	0.354	2
0.65	23.94	53.1	130.85	46.26	0.354	2
0.60	25.59	52.8	142.16	47.28	0.333	1
0.55	24.56	53.1	137.18	47.01	0.343	1
0.50	24.60	53.2	135.93	47.05	0.346	1
0.45	24.07	52.8	132.27	47.46	0.359	1
0.40	24.00	52.8	132.60	47.57	0.359	1
0.35	31.35	52.8	170.40	50.84	0.298	0
			Mesh 90 × 30			
1.00	22.05	53.2	142.25	46.31	0.326	5
0.90	21.48	53.1	142.25	46.48	0.327	4
0.80	22.19	53.2	144.09	47.17	0.327	2
0.70	23.29	53.2	146.48	47.31	0.323	2
0.60	24.13	53.2	155.68	47.75	0.307	1
0.50	23.93	53.2	155.37	48.03	0.309	1
0.40	23.22	53.0	151.79	48.36	0.319	1
0.30	32.38	53.2	202.35	50.96	0.252	0
			Mesh 120 × 40			
1.00	21.29	53.1	188.42	46.72	0.248	6
0.90	21.68	53.1	188.49	47.04	0.250	4
0.80	21.84	53.1	188.31	47.28	0.251	3
0.70	21.57	53.1	189.22	47.32	0.250	3
0.60	23.94	53.0	188.49	48.45	0.257	1
0.50	22.99	53.1	188.47	48.42	0.257	1
0.40	23.37	53.0	188.46	49.00	0.260	1
0.30	29.54	53.0	220.45	51.91	0.235	0

the optimalities of the same mesh density solutions are equivalent, and no significant differences are observed. This indicates that all topologies with varying number of cavities are valid in satisfying the design requirements. Also note that the same number of cavities can be obtained for a range of Γ values.

Conclusions

This paper presented the development of ICC based on ESO to determine an optimal topology with a predefined number of cavities. It has been demonstrated that delaying cavity initiation during optimization using the cavity creation number Γ can control the number of cavities in an optimal topology.

It has been recognized in this study that there are a few optimization parameters that affect the number of cavities. The parameters observed to have direct influences on the number of cavities were the ESO driving criterion, mesh density, and Γ. It was seen that using the maximum VM stresses was more mesh dependent than the mean value.

One contributing factor to mesh dependency of ESO is the size of the elements. As the element size decreases, ESO is able to remove a smaller amount of material at each iteration. This allows for a greater number of cavities in a solution; hence, the number of cavities in the optimal topologies increases as the mesh density increases.

Γ is a newly introduced parameter in ICC to control when a cavity is to be initiated, where $\Gamma = 1.0$ sets the optimization method to original ESO, creating the maximum optimal number of cavities, and $\Gamma = 0.0$ sets to nibbling ESO, creating no cavities. It was displayed that increasing the Γ value also increased the number of cavities, as intended. It was confirmed that topologies of an equivalent optimality with a varied number of cavities could be determined by varying Γ.

The general trends obtained in this study offer a guide for selecting these parameters for a desired number of cavities on a trial-and-error basis. It was observed that the same number of cavities with little or no difference in topology could be obtained for a range of Γ values. Therefore, with the knowledge of selecting the mesh density for a typical FEA problem, one may obtain an optimal topology with a desired number of cavities in one or a few iterations of ICC.

References

[1] Bendsøe, M. P., *Optimization of Structural Topology, Shape and Material*, Springer-Verlag, Berlin, 1995.

[2] Xie, Y. M., and Steven, G. P., *Evolutionary Structural Optimization*, Springer-Verlag, Berlin, 1997.

[3] Fuchs, M. B., Paley, M., and Miroshny, E., "The Aboudi Micromechanical Model for Topology Design of Structures," *Computers and Structures*, Vol. 73, No. 1–5, 1999, pp. 355–362.

[4] Allaire, G., and Kohn, R. V., "Topology Optimization and Optimal Shape Design Using Homogenisation," *Topology Design of Structures*, edited by M. P. Bendsøe and C. A. Mota Soares, Kluwer, Dordrecht, The Netherlands, 1993, pp. 207–218.

[5] Zhou, M., and Rozvany, G. I. N., "The COC Algorithm, Part II: Topological, Geometry and Generalized Shape Optimization," *Computer Methods in Applied Mechanics and Engineering*, Vol. 89, No. 1–3, 1991, pp. 197–224.

[6] Querin, O. M., Steven, G. P., and Xie, Y. M., "Evolutionary Structural Optimisation Using a Bidirectional Algorithm," *Engineering Computations*, Vol. 15, No. 8, 1998, pp. 1031–1048.

[7] Bulman, S., and Hinton, E., "Comparisons Between Algorithms for Structural Topology Optimization Using a Series of Benchmark Studies," *Computers and Structures*, Vol. 79, No. 12, 2001, pp. 1203–1218.

[8] Reynolds, D., McConnachie, J., Bettess, P., Christie, W. C., and Bull, J. W., "Reverse Adaptivity—A New Evolutionary Tool for Structural Optimization," *International Journal for Numerical Methods in Engineering*, Vol. 45, No. 5, 1999, pp. 529–552.

[9] Kim, H., "Vector Formulation of an Optimised Topology for Rapid Prototyping," B. E. Honors Thesis, Dept. of Aeronautical Engineering, Univ. of Sydney, Sydney, NSW, Australia, Nov. 1996.

[10] Hinton, E., Bulman, S., Sienz, J., and Ghasemi, M. R., "Fully Integrated Design Optimization," *Proceedings of the Australasian Conference on Structural Optimisation*, Oxbridge, Victoria, Australia, 1998, pp. 3–29.

[11] Díaz, A., and Sigmund, O., "Checkerboard Patterns in Layout Optimization," *Structural Optimization*, Vol. 10, No. 1, 1995, pp. 40–45.

[12] Jog, C. S., and Haber, R. B., "Stability of Finite Element Models for Distributed-Parameter Optimization and Topology Design," *Computer Methods in Applied Mechanics and Engineering*, Vol. 130, No. 3–4, 1996, pp. 203–226.

[13] Sigmund, O., and Petersson, J., "Numerical Instabilities in Topology Optimization: A Survey on Procedures Dealing with Checkerboards, Mesh-Dependencies and Local Minima," *Structural Optimization*, Vol. 16, No. 1, 1998, pp. 68–75.

[14] Sigmund, O., "On the Design of Compliant Mechanisms Using Topology Optimization," *Mechanics of Structures and Machines*, Vol. 25, No. 4, 1997, pp. 493–524.

[15] Swan, C. C., and Kosaka, I., "Voigt–Reuss Topology Optimisation for Structures with Linear Elastic Material Behaviours," *International Journal for Numerical Methods in Engineering*, Vol. 40, No. 16, 1997, pp. 3033–3057.

[16] Youn, S., and Park, S., "A Study on the Shape Extraction Process in the Structure Topology Optimization Using Homogenized Material," *Computers and Structures*, Vol. 62, No. 3, 1997, pp. 527–538.

[17] Zhou, M., Shyy, Y. K., and Thomas, H. L., "Checkerboard and Minimum Member Size Control in Topology Optimization," *Proceedings of the 3rd World Congress of Structural and Multidisciplinary Optimization* [CD-ROM], Amherst, NY, 1999.

[18] Petersson, J., and Sigmund, O., "Slope Constrained Topology Optimization," *International Journal for Numerical Methods in Engineering*, Vol. 41, No. 8, 1998, pp. 1417–1434.

[19] Haber, R. B., Jog, C. S., and Bendsøe, M. P., "A New Approach to Variable-Topology Shape Design Using a Constraint on Perimeter," *Structural Optimization*, Vol. 11, No. 1–2, 1996, pp. 1–12.

[20] Fernandes, P., Guedes, J. M., and Rodrigues, H., "Topology Optimization of Three-Dimensional Linear Elastic Structures with a Constraint on 'Perimeter'," *Computers and Structures*, Vol. 73, No. 6, 1999, pp. 583–592.

[21] Kim, H., Querin, O. M., Steven, G. P., and Xie, Y. M., "A Method for Varying the Number of Cavities in an Optimised Topology Using Evolutionary Structural Optimisation," *Structural and Multidisciplinary Optimization*, Vol. 19, No. 2, 2000, pp. 140–147.

[22] Xie, Y. M., and Steven, G. P., "Shape and Layout Optimisation via an Evolutionary Procedure," *Proceedings of International Conference on Computational Engineering Science*, Hong Kong, 1992.

A. Messac
Associate Editor